

DESIGN STUDY AROUND BEAM WINDOW OF ADS

**Hiroyuki Oigawa, Kazufumi Tsujimoto, Kenji Kikuchi, Yuji Kurata, Toshinobu Sasa,
Makoto Umeno, Kenji Nishihara, Shigeru Saito, Motoharu Mizumoto, Hideki Takano**
Japan Atomic Energy Research Institute, Japan

Kimikazu Nakai, Azuma Iwata
Mitsubishi Heavy Industries, Ltd., Japan

Abstract

The Japan Atomic Energy Research Institute (JAERI) is conducting the research and development (R&D) on the accelerator-driven subcritical system (ADS) for the effective transmutation of minor actinides (MAs). The ADS proposed by JAERI is an 800 MWth, Pb-Bi cooled, tank-type subcritical reactor loaded with nitride fuel (MA+Pu). Pb-Bi is also used as the spallation target. In this study, the feasibility of the ADS was discussed by focusing on the design around the beam window. The partition wall was placed between the target region and the ductless-type fuel assemblies to keep the good cooling performance for the hot-spot fuel pin. The flow control nozzle was installed to cool the beam window effectively. The thermal-hydraulic analysis showed that the maximum temperature at the outer surface of the beam window could be repressed below 500 C even in the case of maximum beam power (30 MW). The stress caused by the external pressure and the temperature distribution of the beam window was below the allowable limit.

Introduction

To realise the effective transmutation of minor actinides (MA) by an accelerator-driven subcritical system (ADS), a high-power spallation target should be installed at the centre of the core. In the case of JAERI's reference ADS, the proton beam power of ~ 30 MW is necessary to keep the thermal power of the subcritical core at 800 MWth. Such a high-power spallation target is believed to be achievable only by a liquid heavy metal target such as lead-bismuth eutectic (LBE).

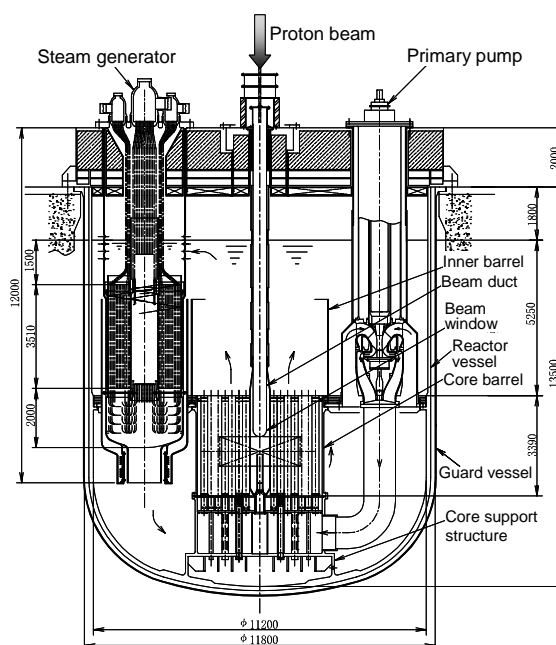
In the design study of ADSs worldwide, two types of spallation targets are proposed – a window type and a windowless type. JAERI has been conducting the design study of the ADS with the beam window, accounting for the difficulty in the stable control of the free surface of the LBE target by the windowless type. Nevertheless, various difficulties arose in the design of the beam window for the high-power spallation target: appropriate cooling, corrosion, structural stress, irradiation damage, etc. In this report, the present status of the design study around the beam window is presented and its feasibility is discussed.

Description of system specification

The subcritical reactor was an 800 MWth, LBE-cooled, tank-type reactor as shown in Figure 1, where LBE was also used as the spallation target. Two primary pumps and four steam generators were contained inside the reactor vessel.

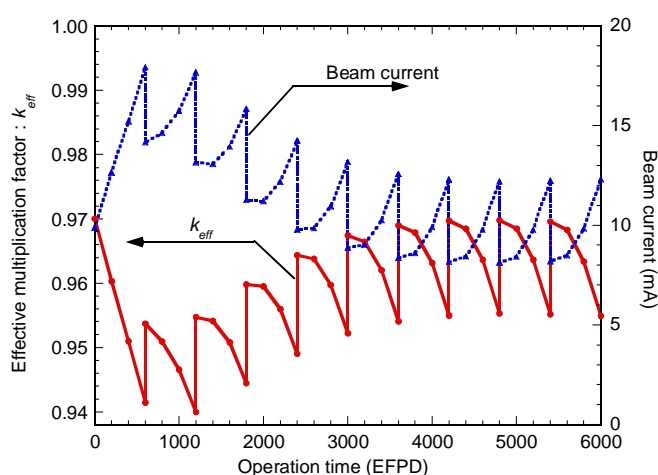
The subcritical core is composed of MA nitride fuel, where plutonium is added at the initial loading of the first cycle to reduce the burn-up swing reactivity. In the reference core design, two-zone fuel loading is adopted to mitigate the high-power peaking factor [1]. The proton energy is set at 1.5 GeV, though it should be optimised in the future considering the trade-off between the cost of the accelerator for higher energy and the engineering difficulty for higher current.

Figure 1. Concept of 800 MWth, LBE-cooled, tank-type ADS



All the fuel in the core was simultaneously unloaded every 600 effective full-power days (EFPD). The unloaded fuel was reprocessed by the pyrochemical method (dry process) to remove the fission products. After the reprocessing, the new nitride fuel was refabricated by adding 250 kg of MA. Figure 2 shows an example of the change of the effective multiplication factor, k_{eff} , according to the fuel burn-up. The maximum value of k_{eff} was set at 0.97, considering reactivity insertion during accidental situations. The plutonium contents in the initial loading fuel were adjusted to 30% and 48% for inner and outer cores, respectively, so that the reactivity swing was minimised. Nevertheless, the minimum k_{eff} of ~ 0.94 was found at the EOC of the second cycle, which means that the burn-up swing reactivity was $\sim 3\%$ Dk. The proton beam current, which kept the thermal power at 800 MW, is shown in Figure 2 where the proton energy was fixed at 1.5 GeV. The maximum beam current of ~ 18 mA (i.e. 27 MW) was necessary at the minimum k_{eff} . During the equilibrium cycles, the beam current was adjusted from 8 to 12 mA (i.e. 12 to 18 MW).

Figure 2. Burn-up reactivity change and required beam current to keep thermal power

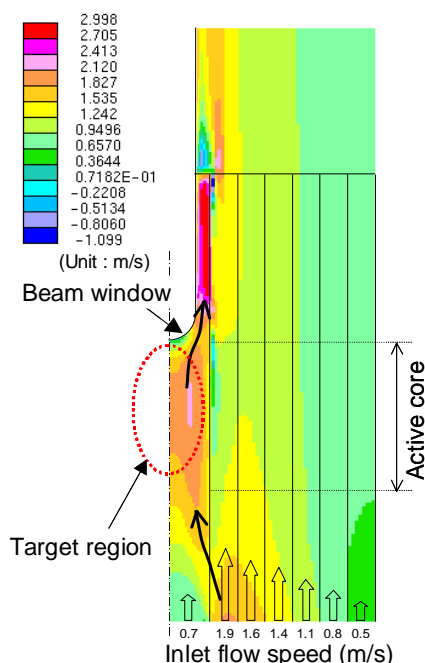


Considering the above-mentioned conditions, we will discuss the feasibility of accepting a 30 MW proton beam. It should be noted that we could reduce the maximum beam current if the temporary low-power operation is acceptable. For example, when we set the limit of the beam current at 15 mA (22.5 MW), the thermal power at the minimum k_{eff} would be ~ 670 MW, which does not seem so serious a deterioration of the system performance.

Preliminary design around beam window

In JAERI's reference design of the ADS, ductless-type fuel assemblies were adopted to reduce the core size, the amount of the waste and neutron capture reactions, and to enhance the cooling capability. In the design around the beam window and the core, LBE was distributed to the target region and the core region at the bottom of the core. In the preliminary design without any wall between the target region and the fuel region, the thermal-hydraulic analysis showed that the cross flow of LBE between these regions occurred as shown in Figure 3 (where the inlet flow speed for each fuel assembly and the target region was determined according to the power density of each region). The observed cross flow deteriorated the flow speed of LBE around the innermost fuel and hence the cooling performance of the hot-spot fuel pins was seriously affected. In addition, the temperature of the beam window became more than 700 C in the case of a sharply peaked proton beam with Gaussian distribution.

Figure 3. Hydraulic analysis for preliminary design without partition wall and inlet nozzle



From this preliminary analysis, the following strategies were considered to find the solution: 1) a partition wall between the target region and the fuel region is necessary to keep the good cooling performance for the fuel pin, 2) the flow distribution among the fuel assemblies is not easy when the ductless-type configuration is adopted, 3) a flow control nozzle is necessary to cool the beam window effectively and 4) other parameters such as the coolant inlet temperature, beam duct diameter and the size of the target region should be optimised. The current design around the beam window derived from the above considerations is shown in the next section.

Modification of design around beam window

The inlet LBE temperature for both the target and the core coolant was reduced to 300 C, while 330 C was adopted in the former design. Although this reduction in temperature may have a negative effect on the power generation efficiency, it is still considered in the acceptable range. The diameter of the beam duct was also expanded from 40 cm to 45 cm to reduce the peak power of the proton beam, though this expansion of the target region deteriorates the neutron economy.

The flow speed of LBE in the core region was set at 2 m/s uniformly to avoid cross flow. But, the erosion and corrosion of fuel claddings by LBE at this flow speed should be examined experimentally. The flow speed of LBE in the flow control nozzle for the target inlet was also set at 2 m/s.

The resultant concept of the spallation target and the core regions is shown in Figure 4. The detail of the design around the beam window is shown in Figure 5. The minimum and maximum gap distances between the beam duct and the partition wall were 1.1 cm and 9.5 cm, respectively. The detailed description of the beam window shape is shown in Figure 6. The thickness of the beam window is 2.0 mm at the centre part and 4.0 mm at the waist part. These two parts should be smoothly connected so as to avoid stress concentration. The thickness of the beam duct is 10 mm.

Figure 4. Design concept of the spallation target and core regions

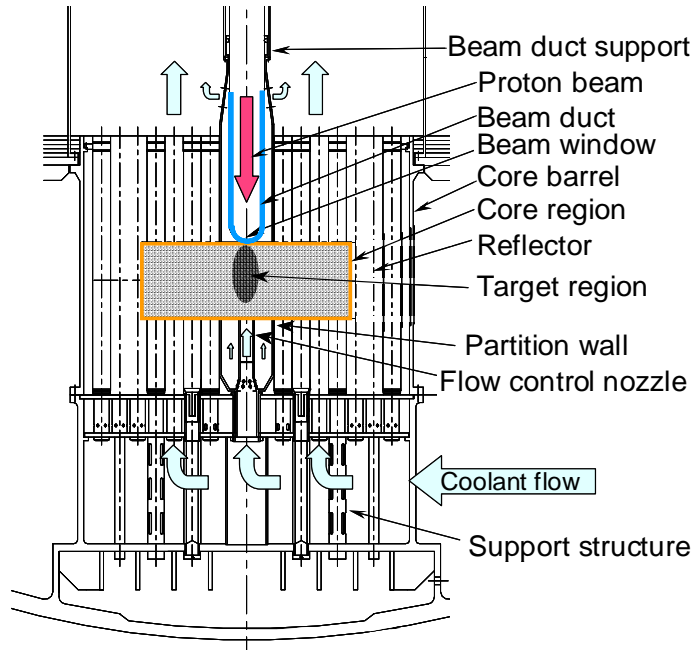


Figure 5. Current design around beam window

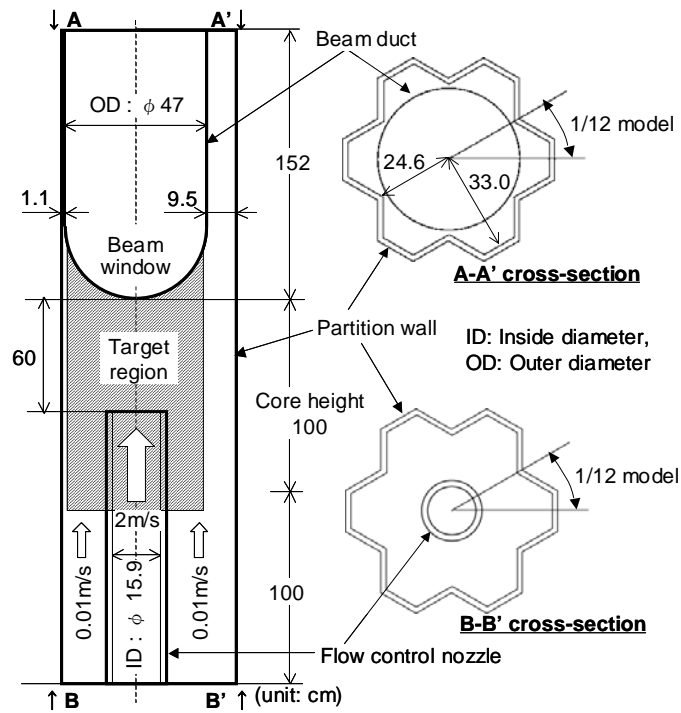
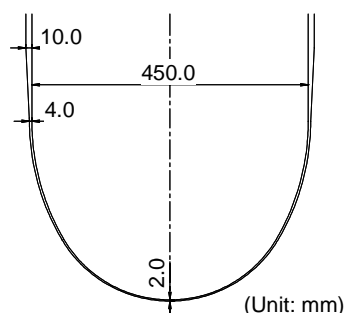


Figure 6. Detailed description of beam window design



The selection of material to be used for the beam window may be one of the toughest issues in the design of the ADS because many factors should be taken into consideration: compatibility with LBE, irradiation effect, strength in high temperature, creep rupture strength, workability, etc. Two candidates were chosen in the meantime – HCM12A and F82H. Characteristics of these materials are summarised in Table 1. The material properties of HCM12A were used in the analysis described below.

Table 1. Characteristics of material chosen temporarily as candidates for beam window (at 550 C)

	HCM12A (Ferritic steel)	F82H (Martensitic steel)
Composition Fe/Cr/W (%)	86/12/2	90/8/2
Tensile strength (MPa)	397	408
Yield stress (MPa)	333	348
Young's modulus (MPa)	$16.6 \cdot 10^4$	$18.3 \cdot 10^4$
Poisson's ratio (-)	0.31	0.30
Thermal expansion coefficient (/K)	$13.4 \cdot 10^{-6}$	$12.2 \cdot 10^{-6}$
Heat conductivity (W/m/K)	29.5	32.2

Thermal-hydraulic analysis of target region

To validate the effect of the above-mentioned design modification, thermal-hydraulic analysis was carried out for the target region. The input beam was $1.5 \text{ GeV} \cdot 20 \text{ mA} = 30 \text{ MW}$ with Gaussian distribution. The deposited heat generation by the beam was calculated as 15.7 MW. The maximum beam density at the centre of the beam window was 30 mA/cm^2 , which caused the heat deposit density of $\sim 700 \text{ W/cm}^3$ in the structural material of the beam window.

Figure 7 shows the results of the hydraulic analysis while Figure 8 shows the temperature analysis. The flow control nozzle is beneficial for effective cooling of the beam window as shown in Figure 7. It should be noted that there will be a stagnant zone at the centre of the beam window when the axially symmetric design is adopted as the present design. Figure 8, however, shows the good cooling performance by such a symmetric design; the outer surface temperature at the centre of the beam window was $\sim 450 \text{ C}$. The maximum temperature at the outer surface of the beam window was found at the peripheral region of the window, instead of at the centre, and its value was $\sim 490 \text{ C}$. It is said that the corrosion of steel alloy by LBE becomes serious above 500 C , though this tendency largely depends on the composition and the surface conditions of the materials and the temperature, as well as on the flow speed and the oxygen concentration of LBE. The present design, therefore, can be regarded as feasible in terms of material corrosion.

Figure 7. Result of hydraulic analysis for beam window

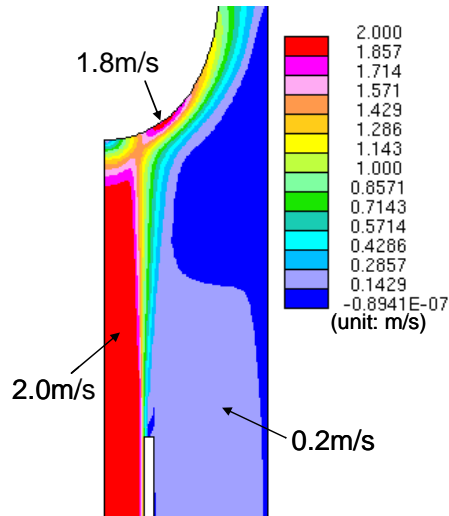
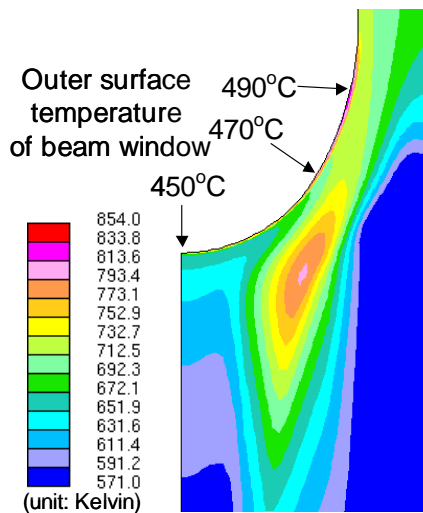


Figure 8. Result of temperature analysis for LBE target and beam window



Structural analysis of beam window

The beam window was under stress by several forces such as: external pressure caused by the hydraulic head of LBE (~680 kPa), cover gas (~100 kPa) and kinetic force of LBE flow (~20 kPa), and thermal stress mainly caused by the temperature difference between the inner and outer surfaces of the beam window. Figure 9 shows the calculated temperature distributions at the inner and outer surfaces of the beam window and the coolant LBE. The maximum temperature difference between the inner and outer surfaces (~50 C) was found at the centre of the beam window. The thermal stress caused by this temperature difference was compressive stress at the inner surface and tensile stress at the outer surface. Since the external pressure caused the compressive stress on both surfaces, the total stress became larger on the inner surface. The resultant Mises stress distributes as shown in Figure 10. The maximum value (~106 MPa) was found at the centre of the beam window. This stress is well below 1/3 of tensile strength shown in Table 1 and therefore the beam window can be judged as feasible from the viewpoint of stress.

Figure 9. Position-dependent temperature of beam window and coolant LBE

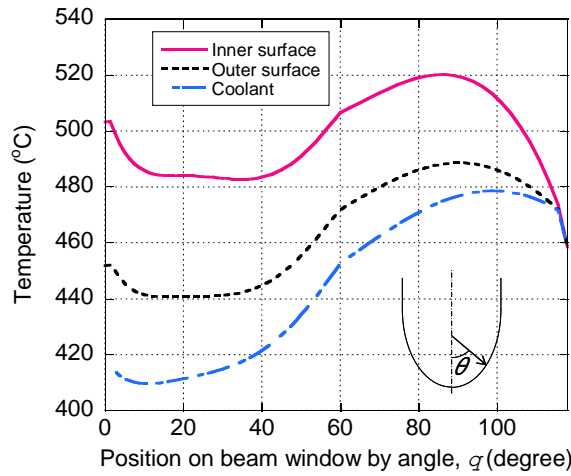
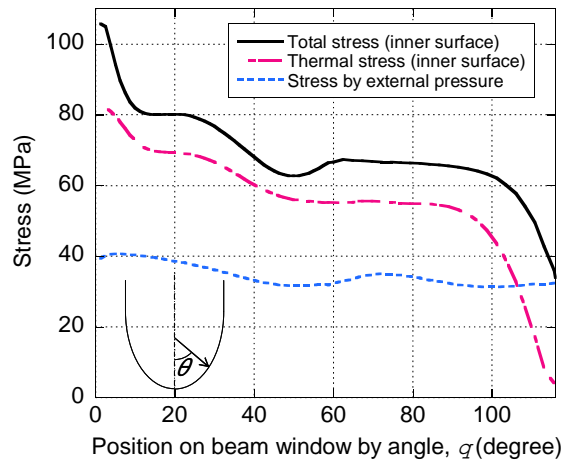


Figure 10. Position-dependent stress caused by temperature difference and external pressure



In addition to this analysis, compression buckling was also analysed. The results showed that compression buckling would result from external pressure of 3.8 MPa, which is more than four times the expected external pressure (0.8 MPa). As for creep, ~0.03% of creep strain was expected even for the 10 000 hours of 120 MPa stress at 520 C. These analyses show that the feasibility of the beam window can be established if the material properties are not seriously deteriorated by the irradiation damage caused by neutrons and protons.

Consideration of other factors

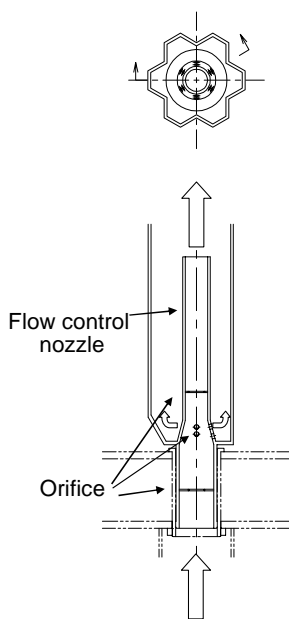
The beam window is heavily exposed by protons and neutrons. The irradiation damage of the beam window was calculated as ~72 DPA (displacement per atom) by neutrons and 6 DPA by protons for a 300-EFPD operation. The helium production was calculated as ~0.15 at.% for the same operation period. To validate the feasibility of the material, therefore, it is essential to accumulate the irradiation data for candidate materials. It should be noted that the combination of neutron irradiation in fast neutron reactors and proton irradiation in the spallation condition is necessary to understand the duplicated effect of heavy irradiation and helium accumulation. The beam window would be exchanged

every one or two years. The partition wall and flow control nozzle would also be exchanged periodically because they too suffer from heavy irradiation. Thus, further study in order to estimate the lifetime of the beam window is a necessary next step.

In the hydraulic analysis described in the previous section, it was assumed appropriate to set the flow rate of the target LBE at the given value. In the design of the whole system, however, how to distribute the flow rate for the core and target regions is one of the technical issues to be developed. A preliminary concept for the target region is shown in Figure 11. Orifices are placed to control the flow rate of the LBE. In the present design where the primary pumps are commonly used for both the core coolant and the target, it is not possible to adjust the flow rate of the target by the pump power (though the beam power should be changed to control the core thermal power during the operation). Experimental validation of the flow control mechanism is considered necessary because the LBE may erode the orifices and change its dimension during the operation.

In the present design concept, contamination of the primary circulation system by spallation products is a concern. This issue remains to be solved in a further study in connection with the development of the polonium management technique.

Figure 11. Concept of flow control mechanism for LBE target



Conclusion

The present conceptual design of an 800 MWth ADS with LBE target/coolant was described and its feasibility was discussed by focusing on the design of the beam window. The partition wall was placed between the target region and the ductless-type fuel assemblies to keep the good cooling performance for the hot-spot fuel pin. A flow control nozzle was installed to effectively cool the beam window. The thermal-hydraulic analysis showed that the maximum temperature at the outer surface of the beam window would be lower than 500 C even in the case of maximum beam power of 30 MW. The stress caused by external pressure and temperature distribution of the beam window was calculated as 106 MPa, which was below 1/3 of the tensile strength of the material.

Further study, including experimental validation, is considered necessary for some technical issues such as: irradiation damage to the beam window, the flow control mechanism for the core and the target regions, and management of spallation products and polonium.

Acknowledgements

This work was funded by the Ministry of Education, Culture, Sports, Science and Technology (MEXT) as one of the R&D programmes for innovative nuclear systems.

REFERENCE

- [1] Tsujimoto, K., *et al.*, “Neutronics Design for Lead-bismuth Cooled Accelerator-driven System for Transmutation of Minor Actinide”, *J. Nucl. Sci. Technol.*, 41, 21 (2004).

TABLE OF CONTENTS

Foreword	3
Executive Summary.....	11
Welcome.....	15
<i>D-S. Yoon</i> Congratulatory Address	17
<i>I-S. Chang</i> Welcome Address	19
<i>G.H. Marcus</i> OECD Welcome	21
GENERAL SESSION: ACCELERATOR PROGRAMMES AND APPLICATIONS.....	23
<i>CHAIRS: B-H. CHOI, R. SHEFFIELD</i>	
<i>T. Mukaiyama</i> Background/Perspective.....	25
<i>M. Salvatores</i> Accelerator-driven Systems in Advanced Fuel Cycles	27
<i>S. Noguchi</i> Present Status of the J-PARC Accelerator Complex	37
<i>H. Takano</i> R&D of ADS in Japan.....	45
<i>R.W. Garnett, A.J. Jason</i> Los Alamos Perspective on High-intensity Accelerators.....	57
<i>J-M. Lagniel</i> French Accelerator Research for ADS Developments.....	69
<i>T-Y. Song, J-E. Cha, C-H. Cho, C-H. Cho, Y. Kim, B-O. Lee, B-S. Lee, W-S. Park, M-J. Shin</i> Hybrid Power Extraction Reactor (HYPER) Project	81

<i>V.P. Bhatnagar, S. Casalta, M. Hugon</i> Research and Development on Accelerator-driven Systems in the EURATOM 5 th and 6 th Framework Programmes.....	89
<i>S. Monti, L. Picardi, C. Rubbia, M. Salvatores, F. Troiani</i> Status of the TRADE Experiment.....	101
<i>P. D'hondt, B. Carlucci</i> The European Project PDS-XADS “Preliminary Design Studies of an Experimental Accelerator-driven System”.....	113
<i>F. Groeschel, A. Cadiou, C. Fazio, T. Kirchner, G. Laffont, K. Thomsen</i> Status of the MEGAPIE Project.....	125
<i>P. Pierini, L. Burgazzi</i> ADS Accelerator Reliability Activities in Europe	137
<i>W. Gudowski</i> ADS Neutronics	149
<i>P. Coddington</i> ADS Safety	151
<i>Y. Cho</i> Technological Aspects and Challenges for High-power Proton Accelerator-driven System Application.....	153
TECHNICAL SESSION I: ACCELERATOR RELIABILITY.....	163
<i>CHAIRS: A. MUELLER, P. PIERINI</i>	
<i>D. Vandeplasseche, Y. Jongen (for the PDS-XADS Working Package 3 Collaboration)</i> The PDS-XADS Reference Accelerator	165
<i>N. Ouchi, N. Akaoka, H. Asano, E. Chishiro, Y. Namekawa, H. Suzuki, T. Ueno, S. Noguchi, E. Kako, N. Ohuchi, K. Saito, T. Shishido, K. Tsuchiya, K. Ohkubo, M. Matsuoka, K. Sennyu, T. Murai, T. Ohtani, C. Tsukishima</i> Development of a Superconducting Proton Linac for ADS.....	175
<i>C. Miélot</i> Spoke Cavities: An Asset for the High Reliability of a Superconducting Accelerator; Studies and Test Results of a $\beta = 0.35$, Two-gap Prototype and its Power Coupler at IPN Orsay	185
<i>X.L. Guan, S.N. Fu, B.C. Cui, H.F. Ouyang, Z.H. Zhang, W.W. Xu, T.G. Xu</i> Chinese Status of HPPA Development	195

<i>J.L. Biarrotte, M. Novati, P. Pierini, H. Safa, D. Uriot</i> Beam Dynamics Studies for the Fault Tolerance Assessment of the PDS-XADS Linac	203
<i>P.A. Schmelzbach</i> High-energy Beat Transport Lines and Delivery System for Intense Proton Beams	215
<i>M. Tanigaki, K. Mishima, S. Shiroya, Y. Ishi, S. Fukumoto, S. Machida, Y. Mori, M. Inoue</i> Construction of a FFAG Complex for ADS Research in KURRI	217
<i>G. Ciavola, L. Celona, S. Gammino, L. Andò, M. Presti, A. Galatà, F. Chines, S. Passarello, XZh. Zhang, M. Winkler, R. Gobin, R. Ferdinand, J. Sherman</i> Improvement of Reliability of the TRASCO Intense Proton Source (TRIPS) at INFN-LNS	223
<i>R.W. Garnett, F.L. Krawczyk, G.H. Neuschaefer</i> An Improved Superconducting ADS Driver Linac Design.....	235
<i>A.P. Durkin, I.V. Shumakov, S.V. Vinogradov</i> Methods and Codes for Estimation of Tolerance in Reliable Radiation-free High-power Linac	245
<i>S. Henderson</i> Status of the Spallation Neutron Source Accelerator Complex	257
TECHNICAL SESSION II: TARGET, WINDOW AND COOLANT TECHNOLOGY.....	265
CHAIRS: X. CHENG, T-Y. SONG	
<i>Y. Kurata, K. Kikuchi, S. Saito, K. Kamata, T. Kitano, H. Oigawa</i> Research and Development on Lead-bismuth Technology for Accelerator-driven Transmutation System at JAERI	267
<i>P. Michelato, E. Bari, E. Cavaliere, L. Monaco, D. Sertore, A. Bonucci, R. Giannantonio, L. Cinotti, P. Turroni</i> Vacuum Gas Dynamics Investigation and Experimental Results on the TRASCO ADS Windowless Interface	279
<i>J-E. Cha, C-H. Cho, T-Y. Song</i> Corrosion Tests in the Static Condition and Installation of Corrosion Loop at KAERI for Lead-bismuth Eutectic	291
<i>P. Schuurmans, P. Kupschus, A. Verstrepen, J. Cools, H. Ait Abderrahim</i> The Vacuum Interface Compatibility Experiment (VICE) Supporting the MYRRHA Windowless Target Design	301

<i>C-H. Cho, Y. Kim, T-Y. Song</i> Introduction of a Dual Injection Tube for the Design of a 20 MW Lead-bismuth Target System.....	313
<i>H. Oigawa, K. Tsujimoto, K. Kikuchi, Y. Kurata, T. Sasa, M. Umeno, K. Nishihara, S. Saito, M. Mizumoto, H. Takano, K. Nakai, A. Iwata</i> Design Study Around Beam Window of ADS.....	325
<i>S. Fan, W. Luo, F. Yan, H. Zhang, Z. Zhao</i> Primary Isotopic Yields for MSDM Calculations of Spallation Reactions on ²⁸⁰ Pb with Proton Energy of 1 GeV.....	335
<i>N. Tak, H-J. Neitzel, X. Cheng</i> CFD Analysis on the Active Part of Window Target Unit for LBE-cooled XADS.....	343
<i>T. Sawada, M. Orito, H. Kobayashi, T. Sasa, V. Artisyuk</i> Optimisation of a Code to Improve Spallation Yield Predictions in an ADS Target System.....	355
TECHNICAL SESSION III: SUBCRITICAL SYSTEM DESIGN AND ADS SIMULATIONS.....	363
<i>CHAIRS: W. GUDOWSKI, H. OIGAWA</i>	
<i>T. Misawa, H. Unesaki, C.H. Pyeon, C. Ichihara, S. Shiroya</i> Research on the Accelerator-driven Subcritical Reactor at the Kyoto University Critical Assembly (KUCA) with an FFAG Proton Accelerator.....	365
<i>K. Nishihara, K. Tsujimoto, H. Oigawa</i> Improvement of Burn-up Swing for an Accelerator-driven System	373
<i>S. Monti, L. Picardi, C. Ronsivalle, C. Rubbia, F. Troiani</i> Status of the Conceptual Design of an Accelerator and Beam Transport Line for Trade.....	383
<i>A.M. Degtyarev, A.K. Kalugin, L.I. Ponomarev</i> Estimation of some Characteristics of the Cascade Subcritical Molten Salt Reactor (CSMSR).....	393
<i>F. Roelofs, E. Komen, K. Van Tichelen, P. Kupschus, H. Ait Abderrahim</i> CFD Analysis of the Heavy Liquid Metal Flow Field in the MYRRHA Pool.....	401
<i>A. D'Angelo, B. Arien, V. Sobolev, G. Van den Eynde, H. Ait Abderrahim, F. Gabrielli</i> Results of the Second Phase of Calculations Relevant to the WPPT Benchmark on Beam Interruptions	411

TECHNICAL SESSION IV: SAFETY AND CONTROL OF ADS 423

CHAIRS: J-M. LAGNIEL, P. CODDINGTON

*P. Coddington, K. Mikityuk, M. Schikorr, W. Maschek,
R. Sehgal, J. Champigny, L. Mansani, P. Meloni, H. Wider*
Safety Analysis of the EU PDS-XADS Designs..... 425

*X-N. Chen, T. Suzuki, A. Rineiski, C. Matzerath-Boccaccini,
E. Wiegner, W. Maschek*
Comparative Transient Analyses of Accelerator-driven Systems
with Mixed Oxide and Advanced Fertile-free Fuels 439

P. Coddington, K. Mikityuk, R. Chawla
Comparative Transient Analysis of Pb/Bi
and Gas-cooled XADS Concepts 453

B.R. Sehgal, W.M. Ma, A. Karbojian
Thermal-hydraulic Experiments on the TALL LBE Test Facility 465

K. Nishihara, H. Oigawa
Analysis of Lead-bismuth Eutectic Flowing into Beam Duct..... 477

P.M. Bokov, D. Ridikas, I.S. Slessarev
On the Supplementary Feedback Effect Specific
for Accelerator-coupled Systems (ACS)..... 485

W. Haeck, H. Ait Abderrahim, C. Wagemans
 K_{eff} and K_s Burn-up Swing Compensation in MYRRHA 495

TECHNICAL SESSION V: ADS EXPERIMENTS AND TEST FACILITIES 505

CHAIRS: P. D'HONDT, V. BHATNAGAR

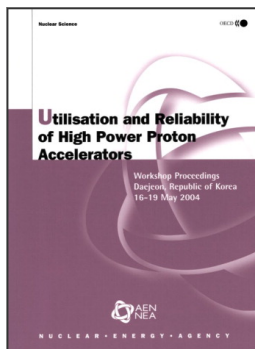
*H. Oigawa, T. Sasa, K. Kikuchi, K. Nishihara, Y. Kurata, M. Umeno,
K. Tsujimoto, S. Saito, M. Futakawa, M. Mizumoto, H. Takano*
Concept of Transmutation Experimental Facility 507

M. Hron, M. Mikisek, I. Peka, P. Hosnedl
Experimental Verification of Selected Transmutation Technology and Materials
for Basic Components of a Demonstration Transmuter with Liquid Fuel
Based on Molten Fluorides (Development of New Technologies for
Nuclear Incineration of PWR Spent Fuel in the Czech Republic) 519

Y. Kim, T-Y. Song
Application of the HYPER System to the DUPIC Fuel Cycle..... 529

M. Plaschy, S. Pelloni, P. Coddington, R. Chawla, G. Rimpault, F. Mellier
Numerical Comparisons Between Neutronic Characteristics of MUSE4
Configurations and XADS-type Models 539

<i>B-S. Lee, Y. Kim, J-H. Lee, T-Y. Song</i> Thermal Stability of the U-Zr Fuel and its Interfacial Reaction with Lead	549
SUMMARIES OF TECHNICAL SESSIONS	557
<i>CHAIRS: R. SHEFFIELD, B-H. CHOI</i>	
<i>Chairs: A.C. Mueller, P. Pierini</i> Summary of Technical Session I: Accelerator Reliability	559
<i>Chairs: X. Cheng, T-Y. Song</i> Summary of Technical Session II: Target, Window and Coolant Technology	565
<i>Chairs: W. Gudowski, H. Oigawa</i> Summary of Technical Session III: Subcritical System Design and ADS Simulations.....	571
<i>Chairs: J-M. Lagniel, P. Coddington</i> Summary of Technical Session IV: Safety and Control of ADS	575
<i>Chairs: P. D'hondt, V. Bhatagnar</i> Summary of Technical Session V: ADS Experiments and Test Facilities.....	577
SUMMARIES OF WORKING GROUP DISCUSSION SESSIONS	581
<i>CHAIRS: R. SHEFFIELD, B-H. CHOI</i>	
<i>Chair: P.K. Sigg</i> Summary of Working Group Discussion on Accelerators.....	583
<i>Chair: W. Gudowski</i> Summary of Working Group Discussion on Subcritical Systems and Interface Engineering	587
<i>Chair: P. Coddington</i> Summary of Working Group Discussion on Safety and Control of ADS.....	591
<i>Annex 1: List of workshop organisers</i>	<i>595</i>
<i>Annex 2: List of participants.....</i>	<i>597</i>



From:

Utilisation and Reliability of High Power Proton Accelerators

Workshop Proceedings, Daejeon, Republic of Korea, 16-19 May 2004

Access the complete publication at:

<https://doi.org/10.1787/9789264013810-en>

Please cite this chapter as:

Oigawa, Hiroyuki, *et al.* (2006), "Design Study around Beam Window of ADS", in OECD/Nuclear Energy Agency, *Utilisation and Reliability of High Power Proton Accelerators: Workshop Proceedings, Daejeon, Republic of Korea, 16-19 May 2004*, OECD Publishing, Paris.

DOI: <https://doi.org/10.1787/9789264013810-34-en>

This work is published under the responsibility of the Secretary-General of the OECD. The opinions expressed and arguments employed herein do not necessarily reflect the official views of OECD member countries.

This document and any map included herein are without prejudice to the status of or sovereignty over any territory, to the delimitation of international frontiers and boundaries and to the name of any territory, city or area.

You can copy, download or print OECD content for your own use, and you can include excerpts from OECD publications, databases and multimedia products in your own documents, presentations, blogs, websites and teaching materials, provided that suitable acknowledgment of OECD as source and copyright owner is given. All requests for public or commercial use and translation rights should be submitted to rights@oecd.org. Requests for permission to photocopy portions of this material for public or commercial use shall be addressed directly to the Copyright Clearance Center (CCC) at info@copyright.com or the Centre français d'exploitation du droit de copie (CFC) at contact@cfcopies.com.